AMERICAN SOCIETY FOR MICROBIOLOGY | Molecular and Cellular Biology

A Mutation in the Flavin Adenine Dinucleotide-Dependent Oxidoreductase FOXRED1 Results in Cell-Type-Specific Assembly Defects in Oxidative Phosphorylation Complexes I and II

Olga Zurita Rendón,[a] Hana Antonicka,[a] Rita Horvath,[b] Eric A. Shoubridge[a]

Montreal Neurological Institute and Department of Human Genetics, McGill University, Montreal, Quebec, Canada[a]; Institute of Genetic Medicine, Newcastle University, Newcastle upon Tyne, United Kingdom[b]

Complex I (NADH ubiquinone oxidoreductase) is a large multisubunit enzyme that catalyzes the first step in oxidative phosphorylation (OXPHOS). In mammals, complex I biogenesis occurs in a stepwise manner, a process that requires the participation of several nucleus-encoded accessory proteins. The FAD-dependent oxidoreductase-containing domain 1 (FOXRED1) protein is a complex I assembly factor; however, its specific role in the assembly pathway remains poorly understood. We identified a homozygous missense mutation, c.1308 G→A (p.V421M) in *FOXRED1* in a patient who presented with epilepsy and severe psychomotor retardation. A patient myoblast line showed a severe reduction in complex I, associated with the accumulation of subassemblies centered around ~340 kDa, and a milder decrease in complex II, all of which were rescued by retroviral expression of wild-type FOXRED1. Two additional assembly factors, AIFM1 and ACAD9, coimmunoprecipitated with FOXRED1, and all were associated with a 370-kDa complex I subassembly that, together with a 315-kDa subassembly, forms the 550-kDa subcomplex. Loss of FOXRED1 function prevents efficient formation of this midassembly subcomplex. Although we could not identify subassemblies of complex II, our results establish that FOXRED1 function is both broader than expected, involving the assembly of two flavoprotein-containing OXPHOS complexes, and cell type specific.

The oxidative phosphorylation (OXPHOS) system is responsible for the generation of the majority of cellular ATP. NADH ubiquinone oxidoreductase (complex I), the first enzyme in the pathway, is responsible for the oxidation of NADH. This is coupled with the pumping of protons across the inner mitochondrial membrane, contributing to the formation of the electrochemical gradient that is ultimately used by ATP synthase (complex V) to generate ATP.

Complex I is embedded in the inner mitochondrial membrane, forming an L-shaped structure with a membrane domain and a peripheral domain that protrudes into the mitochondrial matrix. It is composed of 44 structural subunits, 7 of which are encoded by the mitochondrial genome (mitochondrial DNA [mtDNA]). In mammals, complex I biogenesis occurs in a stepwise fashion by sequential addition of assembly intermediates (1). Assembly of the holoenzyme requires the import of the 37 nucleus-encoded subunits, followed by sorting, folding, and assembly into the appropriate structural domain of the complex. Seven iron-sulfur clusters are incorporated into five of the core subunits of the peripheral arm (NDUFS1, NDUFS7, NDUFS8, NDUFV1, and NDUFV2), and a flavin mononucleotide (FMN) molecule is inserted noncovalently into NDUFV1.

Deficiencies in the activity of complex I, among the most common causes of OXPHOS disorders, are associated with a wide variety of clinical phenotypes that can range from lethal infantile diseases to isolated myopathy or adult-onset neurodegenerative disorders (2). Mutational analyses have identified defects in all 14 core subunits and several of the so-called supernumerary subunits of the complex; however, these mutations explain only about 50% of the cases (3, 4), implicating assembly factors as an important cause of disease.

To date, 13 different complex I assembly factors have been identified—NDUFAF1 (CIA30) (5), NDUFAF2 (B17.2L) (6), NDUFAF3 (C3ORF60) (7), NDUFAF4 (C6ORF66) (8), NDUFAF5 (C20ORF7) (9), NDUFAF6 (C8ORF38) (10), Ecsit (11), NDUFAF7 (pro1853) (12), FOXRED1 (13), IND1 (NUBPL) (14), ACAD9 (15), TMEM126B (16), C3orf1 (17), and possibly AIFM1 (18)—yet the exact molecular functions of most of them in complex I biogenesis remain poorly understood. Two independent studies reported isolated complex I deficiency associated with mutations in the FAD-dependent oxidoreductase-containing domain 1 (FOXRED1) protein, demonstrating that FOXRED1 functions in complex I assembly (13, 19). Characterization of fibroblast lines from these patients demonstrated that FOXRED1 is involved in the middle to late stages of complex I assembly (20); however, the precise molecular role of the chaperone remains elusive.

Here, we show that depletion of FOXRED1 in myoblasts results in decreased levels of fully assembled complexes I and II. We demonstrate that FOXRED1 associates with the ND1-containing subcomplexes of ~370 kDa and ~620 kDa and that FOXRED1 activity is required for the formation of a 550-kDa subcomplex of complex I.

Received 29 January 2016 **Returned for modification** 14 February 2016
Accepted 16 May 2016

Accepted manuscript posted online 23 May 2016

Citation Zurita Rendón O, Antonicka H, Horvath R, Shoubridge EA. 2016. A mutation in the flavin adenine dinucleotide-dependent oxidoreductase FOXRED1 results in cell-type-specific assembly defects in oxidative phosphorylation complexes I and II. Mol Cell Biol 36:2132–2140. doi:10.1128/MCB.00066-16.

Address correspondence to Eric A. Shoubridge, eric@ericpc.mni.mcgill.ca.

Supplemental material for this article may be found at http://dx.doi.org/10.1128/MCB.00066-16.

MATERIALS AND METHODS

Identification of the mutation. Sanger sequencing of FOXRED1 in the subject and control cDNAs was performed using the following primers: FR1-F, GCAGCAGTGCAGCTTTCAGAGG; FR1-R, TATTGGCCTCGG CCTCACTGC; FR1-insideF, AGGGAGTGGCTTTGGCGTCTTATGG; and FR1-insideR, ATTCCACAGGCTGGTACTCCAGG.

Cell culture. Primary cell lines were established from myoblasts (Control-1, Control-2, and Patient) and fibroblasts (Control-3) and immortalized by transduction with a retroviral vector expressing the human papillomavirus 16 (HPV-16) E7 gene and the catalytic component of human telomerase (21). The fibroblast lines were grown in high-glucose Dulbecco's modified Eagle medium (DMEM) supplemented with fetal bovine serum (10%). The myoblasts were grown in F-10 medium supplemented with bovine serum albumin (0.5 mg/ml), fetuin (0.5 mg/ml), insulin (0.18 mg/ml), dexamethasone (0.4 μg/ml), mouse epidermal growth factor (10 ng/ml), and fetal bovine serum (15%). All the cell lines were grown at 37°C in an atmosphere of 5% CO_2.

FOXRED1 constructs. To generate the FOXRED1 or the C-terminal Myc-tagged FOXRED1 construct, cDNA was amplified by OneStep reverse transcription (RT)-PCR (Qiagen) using specific primers modified for cloning into Gateway vectors (Invitrogen). The accuracy of the clones was verified by DNA sequencing. Retroviral constructs were transiently transfected into the Phoenix packaging cell line using the HEPES-buffered saline (HBS)–$Ca_3(PO_4)_2$ method. Control or patient cell lines were infected 48 h later by exposure to virus-containing medium in the presence of Polybrene (4 g/ml) as described previously (https://web.stanford.edu/group/nolan/_OldWebsite/protocols/pro_helper_dep.html).

RNAi transfection. For the FOXRED1 knockdown experiments, we used a Stealth RNA interference (RNAi) duplex construct (Invitrogen, Carlsbad, CA): GCUUUCUACGGAACAUCAAUGAGUA. The cell lines were transfected twice, at days 1 and 3, and analyzed at day 6. The constructs were designed using the BLOCK-iT RNAi Express website (http://rnaidesigner.invitrogen.com/rnaiexpress/rnaiExpress.jsp?CID=FL-RNAIEXPRESS). Fibroblasts/myoblasts were transfected using the Lipofectamine RNAiMax protocol in Opti-MEM reduced serum medium. Block-iTAlexa Fluor Red fluorescent oligonucleotide was used to assess the transfection efficiency (transfection performed in parallel with the other Stealth constructs) and as a mock oligonucleotide transfection control (all reagents were from Invitrogen).

SDS-PAGE immunoblot analysis. Whole-cell extracts were prepared by solubilization of pelleted cells at a 1:5 ratio with extraction buffer (1.5% dodecyl maltoside) for 30 min on ice. The soluble fraction was obtained by centrifugation at 20,000 × *g* for 20 min at 4°C. Samples were mixed at a 1:1 ratio with 2× Laemmli loading buffer, and the solubilized proteins were loaded onto a 12% acrylamide-bisacrylamide (29:1) gel. The protein gel was transfer to a nitrocellulose membrane using a wet-transfer system. Subsequent immunoblotting was done with the appropriate antibodies. Antibodies were obtained as follows: MitoSciences, NDUFS2, ATPase α, SDHB, and actin; Abcam, NDUFA9, COX2, UQCRC1, SDHA, ACAD9, and porin; Santa Cruz, AIFM1; and Proteintech, FOXRED1 and ETFB. The ND1 antibody was kindly provided by A. Lombes, and it was used in all the experiments except one (see Fig. 7), where a monoclonal ND1 antibody was used.

BN-PAGE and second-dimension denaturing gel electrophoresis (2D-SDS-PAGE) immunoblot analysis. Mitoplasts were prepared from myoblasts and fibroblasts as described previously (22) by treating the cells with 0.8 mg digitonin/mg of protein. The mitoplasts were solubilized with 1% dodecyl maltoside, and the solubilized proteins were used for electrophoresis. Blue-Native polyacrylamide gel electrophoresis (BN-PAGE) (23) was used to separate the samples in the first dimension on 6 to 15% polyacrylamide gradients. For analysis of the second dimension, strips of the first-dimension gel were incubated for 30 min in 1% SDS and 1% β-mercaptoethanol. These strips were then run on a 10% Tricine–SDS-PAGE gel to separate the proteins in the second dimension (23). Individual structural subunits of complexes I, II, III, and IV were detected by immunoblot analysis using commercially available monoclonal antibodies (MitoSciences and Abcam), except for complex I, where a polyclonal antibody against subunit ND1 was used. FOXRED1 was revealed by immunoblot analysis with polyclonal FOXRED1 antibody (Novus Biologicals). The sizes of the observed subcomplexes (340 kDa and 620 kDa) were determined by their migrations relative to those of the OXPHOS complexes—I (980 kDa), II (123 kDa), III (482 kDa), and IV (205 kDa)—which were used as standards (24).

Size exclusion chromatography. Mitochondrial protein extracts from a control fibroblast line were fractionated on a Tricorn Superdex 200 10/30 HR column (GE Healthcare) as described previously (25), and the elution profile of FOXRED1 was revealed by immunoblot analysis with polyclonal FOXRED1 antibody (Novus Biologicals). The molecular weights of the individual fractions were calculated from the elution profile of a set of standards, including TFAM, LRPPRC, and ND1.

Pulse-labeling of mitochondrial translation products. Labeling of the mitochondrial translation products was performed as previously described (26). Briefly, cells were labeled for 60 min at 37°C in methionine- and cysteine-free DMEM containing 200 μCi/ml [^{35}S]methionine-cysteine and 100 μg/ml emetine, followed by a chase of 10 min in regular DMEM. Protein extraction was done in labeled cells (50 μg) by resuspension in Laemmli loading buffer and sonication for 5 s. Samples were run on 15 to 20% polyacrylamide gradient gels. The labeled mitochondrial translation products were detected by direct autoradiography on a phosphorimager.

Immunoprecipitation experiments and mass spectrometry analysis. Purified mitochondria (800 μg) from the FOXRED1-Myc cell line were extracted on ice in 200 μl of extraction buffer (50 mM HEPES buffer, pH 7.6, 150 mM NaCl, 1% taurodeoxycholate) supplemented with complete protease inhibitors (Roche) for 45 min. The protein extract was centrifuged at 25,000 × *g* at 4°C for 40 min, and the supernatant was used to immunoprecipitate FOXRED1. Immunoprecipitation was performed on magnetic Dynabeads (Life Technologies) according to the manufacturer's instructions. Incubation of the protein extract with the beads was carried out overnight at 4°C. Bound protein was eluted with elution buffer containing 0.1 M glycine (pH 2.5) and 0.5% dodecyl maltoside (DDM) and trichloroacetic acid (TCA) at room temperature, followed by TCA precipitation. The precipitated protein was digested with trypsin and analyzed by mass spectrometry (LTQ Orbitrap Velos; ThermoFisher Scientific, Bremen, Germany) at the Institut de Recherches Cliniques de Montreal, Montreal, Canada.

Mitochondrial isolation and localization experiments. Myoblasts were resuspended in ice-cold SET buffer containing 250 mM sucrose, 10 mM Tris-HCl, and 1 mM EDTA (pH 7.4) and supplemented with Complete protease inhibitors (Roche) and were homogenized with 10 passes through a prechilled, zero clearance homogenizer (Kimble/Kontes). The homogenized cellular extract was then centrifuged twice for 10 min each time at 600 × *g* to obtain a postnuclear supernatant. Mitochondria were pelleted by centrifugation for 10 min at 10,000 × *g* and washed once in the same buffer.

Immunofluorescence analysis was performed using a control cell line overexpressing FOXRED1-Myc. Glass slides were fixed in 4% paraformaldehyde at 50% confluence, followed by 1 h of incubation with Myc and SLIRP (Abcam) antibodies, which preceded the addition of secondary antibodies coupled with Alexa Fluor fluorochromes (Invitrogen). DAPI (4′,6-diamidino-2-phenylindole) was used to stain DNA. Images were obtained with an inverted fluorescence microscope.

Flavination assay. BN samples were resuspended in 2× Laemmli loading buffer and run on an SDS-PAGE gel, followed by 30-min incubation of the protein gel in 10% acetic acid; 520-nm emission by covalently bound flavin adenine dinucleotide (FAD) upon excitation at 450 nm was measured with a Typhoon imager (Amersham Biosciences) (method adapted from references 27 and 28). In parallel, the same samples were transferred to a nitrocellulose membrane. Subsequent immunoblotting was done with the appropriate antibodies.

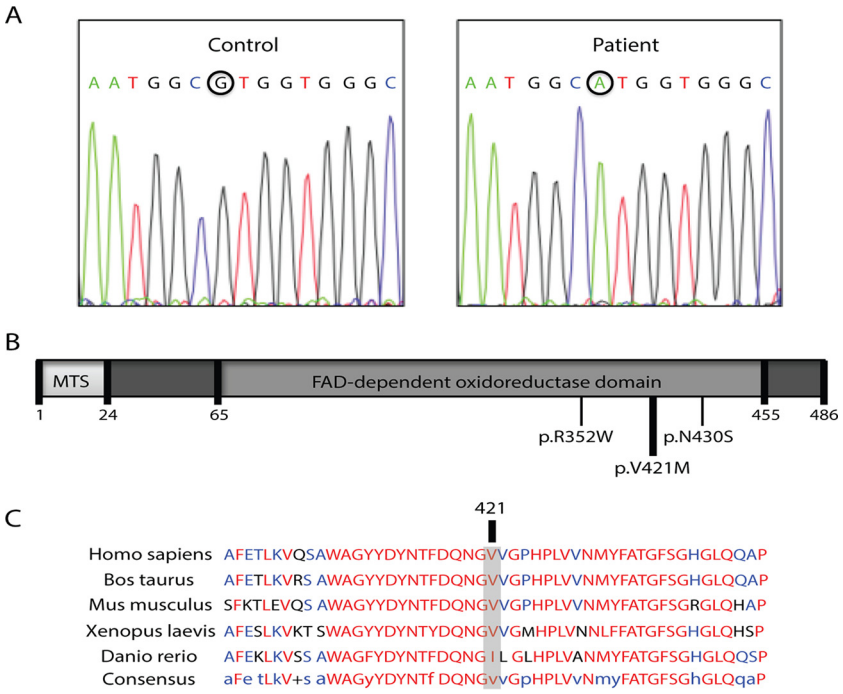

FIG 1 Mutational analysis of FOXRED1. (A) Sequence analysis of FOXRED1 genomic DNA (gDNA) showing the position of the homozygous missense mutation c.1308 G→A identified in the patient compared to the control. (B) FOXRED1 contains a putative mitochondrial targeting sequence (MTS) and a FAD-dependent oxidoreductase domain. The missense mutations in FOXRED1 identified previously and in the present study are indicated by bars. (C) Multiple-sequence alignment of FOXRED1 protein sequences showing that the valine at position 421 is conserved throughout evolution.

Succinate dehydrogenase activity. Control and patient myoblasts were homogenized in 25 mM potassium phosphate buffer, pH 7.4. SDH activity was measured at 25°C in a buffer containing 50 mM potassium phosphate (pH 7.4), 20 mM succinate, 40 μM dichlorophenolindophenol, 3 μg/ml antimycin A, and 1% dodecyl maltoside at 600 nm. Citrate synthase (CS) activity was measured as previously reported (29). SDH activity was normalized to CS and is reported as a percentage of two controls. All activities were measured as three independent biological replicates.

RESULTS

Identification of a mutation in FOXRED1. The initial biochemical characterization of an Iraqi patient presenting with epilepsy and severe psychomotor retardation was done by BN-PAGE in patient fibroblasts and showed an isolated deficiency in complex I (NADH ubiquinone oxidoreductase) (data not shown). The proband had two siblings, one presenting similar clinical features, who died at 8 years of age, and a second, healthy brother. Using a candidate gene approach, we identified a homozygous missense mutation, c.1308 G→A, in the *FOXRED1* gene (Fig. 1A), coding for a protein previously described as required for the assembly of holocomplex I (13, 19). The c.1308 G→A mutation predicts an amino acid substitution, p.V421M (RefSeq accession number NM_017547) (Fig. 1A and B), that is highly conserved among different taxa (Fig. 1C). FOXRED1 (NP_060017.1), is a 53-kDa protein with a predicted mitochondrial targeting sequencing of 24 amino acids (http://ihg.gsf.de/ihg/mitoprot.html) that contains an FAD-dependent oxidoreductase domain (pfam01266:DAO). Missense mutations in the FAD-dependent oxidoreductase domain of FOXRED1 were also identified in the other two reported patients (Fig. 1B).

The p.V421M variant in FOXRED1 leads to a combined deficiency of complexes I and II. To further characterize the complex I deficiency observed in the FOXRED1 patient, we performed a BN-PAGE experiment to evaluate the assembly profile of complex I using an anti-ND1 antibody in control and patient myoblasts. We detected decreased levels of fully assembled complex I, the accumulation of complex I subcomplexes, and, unexpectedly, decreased levels of fully assembled complex II (Fig. 2A). To confirm that the mutation in FOXRED1 was responsible for the assembly defects observed in both complexes I and II, we used a retroviral vector to express a wild-type FOXRED1 cDNA in control and patient myoblasts. Expression of wild-type FOXRED1 rescued the complex I and II deficiencies, confirming that the c.1308 G→A mutation in *FOXRED1* is the cause of the assembly defect in complex I and also suggesting that FOXRED1 is required for complex II assembly in myoblasts (Fig. 2A).

To eliminate the possibility that the complex II deficiency observed in the FOXRED1 patient was the result of a technical artifact, we reran a BN-PAGE experiment using the same samples shown in Fig. 2A, except that the patient sample was loaded with twice the amount of protein as the other samples. Although this showed that the steady-state levels of complex II were compensated for, the steady-state levels of fully assembled complex I remained low compared to controls. An in-gel activity (IGA) assay also confirmed the deficiency of complex I. Moreover, in this analysis, the steady-state levels of complexes III and IV were increased in the patient cell line compared to controls, further supporting the observation that the complex II deficiency is not an artifact (Fig. 2B). Consistently, spectrophotometric measurements of complex II activity in the patient cell line showed an ~40% decrease compared to controls.

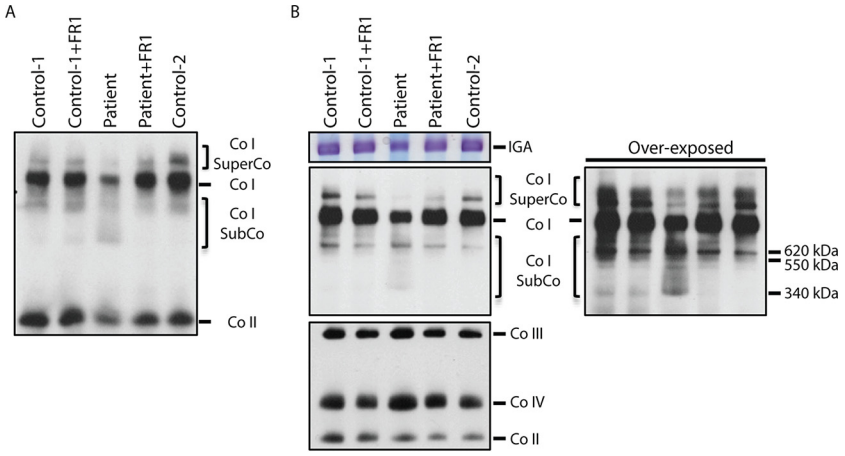

FIG 2 Analysis of the OXPHOS profile in the FOXRED1 patient cell line. (A) BN-PAGE analysis of the FOXRED1 patient cell line (Patient), the patient cell line overexpressing wild-type FOXRED1 (Patient+FR1), and three different controls (Control-1, Control-1+FR1, and Control-2). (B) IGA of complex I and BN-PAGE analysis of the same cell lines shown in panel A, with the patient cell line loaded with twice the total protein of the other samples. On the right is an overexposed image of the ND1 immunoblot showing complex I-containing supercomplexes (Co I SuperCo), holocomplex I (Co I), and the subcomplexes (Co I SubCo) present in the patient cell line. OXPHOS complexes were detected with subunit-specific antibodies: Co I, ND1; Co II, SDHA; Co III, UQCRC1; and Co IV, COX4.

The steady-state levels of FOXRED1 and the structural subunits of complexes I and II were next investigated by immunoblot analysis (Fig. 3A). FOXRED1 was decreased in the patient myoblast line compared to controls, as were the levels of two structural subunits of complex I, NDUFS2 and ND1, which were rescued by retroviral expression of wild-type FOXRED1 (Fig. 3A). We also evaluated the steady-state levels of the complex I assembly factors ACAD9 and AIFM1 by immunoblotting (Fig. 3A), which showed no differences between the patient and controls. The steady-state levels of structural subunits of complex II, SDHA and SDHB, remained unaffected in the patient myoblasts compared to controls (Fig. 3A). The FAD covalently bound to SDHA was also unaffected in the patient myoblasts and in myoblasts treated with a small interfering RNA (siRNA) against FOXRED1 (Fig. 3B).

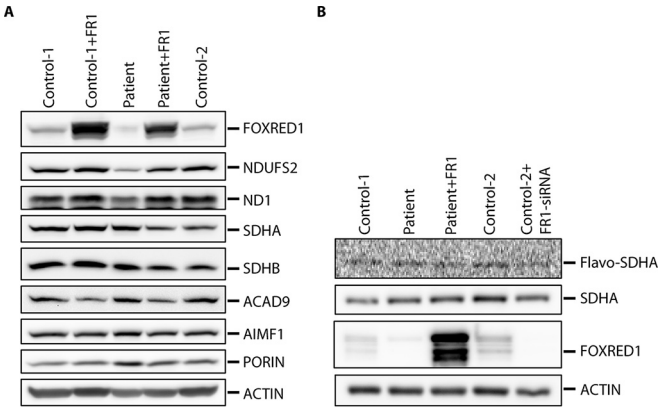

FIG 3 Analysis of the steady-state levels of complex I and II components in FOXRED1-depleted cell lines. (A) SDS-PAGE analysis of the patient (Patient and Patient+FR1) and control (Control-1, Control-1+FR1, and Control-2) cell lines. The immunoblots show the steady-state levels of FOXRED1, complex I (NDUFS2 and ND1), and complex II (SDHA and SDHB) structural subunits; complex I assembly factors (ACAD9 and AIFM1); and loading controls (porin and actin). (B) SDS-PAGE analysis of FOXRED1-depleted cell lines (Patient and Control-2+FR1 siRNA) and controls (Control-1, Patient+FR1, and Control-2) was followed by imaging of covalently bound FAD (Flavo-SDHA) or immunoblotting with the indicated antibodies: complex II structural subunit (SDHA) and FOXRED1 and loading control (actin).

FOXRED1 depletion results in the accumulation of an ~340-kDa subassembly of complex I. Immunodetection of complex I using an ND1 antibody identified three subcomplexes in the FOXRED1 patient myoblast line (Fig. 2B). To determine their molecular masses, we performed a linear regression analysis based on their BN-PAGE migration, using as standards the OXPHOS complexes: I (980 kDa), II (123 kDa), III (482 kDa), and IV (205 kDa) (24). This analysis estimated that the smallest subcomplex corresponded to ~340 kDa, with a second subcomplex of ~550 kDa and a third subcomplex of ~620 kDa. To determine if these subcomplexes were specific to the myoblast lines we analyzed, we used an siRNA construct to deplete FOXRED1 in a fibroblast line. BN-PAGE analysis of the fibroblast control (Control-3) and the FOXRED1-depleted cell line showed that the depletion of FOXRED1 expression results in a severe decrease in the steady-state levels of holocomplex I and the subcomplex of ~550 kDa, while the ~620-kDa subcomplex was only slightly reduced and the ~340-kDa subcomplex accumulated (Fig. 4A). Interestingly, the steady-state levels of fully assembled complex II remained unaffected. To further evaluate the complex II deficiency observed in the FOXRED1 patient myoblast line, we used siRNA to suppress FOXRED1 in the Control-2 myoblast line. BN-PAGE analysis of these two cell lines confirmed that FOXRED1 depletion in myoblasts resulted in decreased levels of both complexes I and II, whereas complex IV remained unaffected (Fig. 4B).

FOXRED1 interacts with complex I subcomplexes of ~370 and ~620 kDa. To further investigate the role of FOXRED1 in the biogenesis of complex I, we performed 2D-SDS-PAGE in the control and FOXRED1 patient myoblasts. This showed that the ~340-kDa subcomplex accumulated in the patient cell line, whereas the 620-kDa subcomplex was slightly decreased relative to the control. 2D-SDS-PAGE analysis of the control and the patient cell lines expressing wild-type FOXRED1 showed that while most FOXRED1 accumulated at a molecular mass corresponding to its monomeric size, a small amount was also detected in two

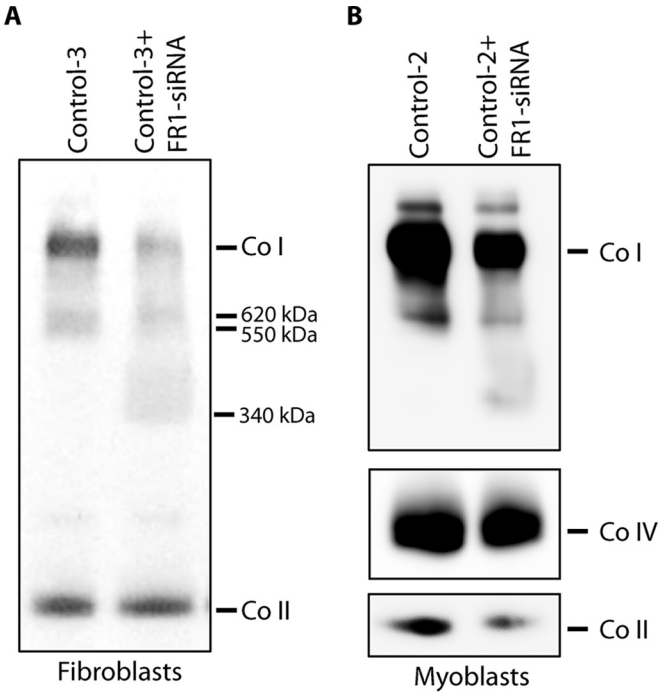

FIG 4 BN-PAGE analysis of FOXRED1-depleted cell lines. FOXRED1 was depleted using siRNA in fibroblasts (Control-3 and Control-3+FOXRED1-siRNA) (A) and myoblasts (Control-2 and Control-2+FOXRED1-siRNA) (B), and OXPHOS complexes were detected with subunit-specific antibodies: Co I, ND1; Co II, SDHA; and Co IV, COX4.

discrete higher-molecular-mass complexes corresponding to ~370 and ~620 kDa (Fig. 5A).

Size exclusion chromatography of a fibroblast control line demonstrated that FOXRED1 was mainly enriched in a fraction corresponding to 70 kDa, with smaller amounts of FOXRED1 centered at ~600 kDa and ~1.8 MDa (Fig. 5B). These results are consistent with the profile observed for FOXRED1 in the 2D-SDS-PAGE experiment and also suggest that FOXRED1 could be associated with and/or involved in the formation of complex I-containing supercomplexes.

Previously, we showed that early assembly defects in complex I biogenesis result in rapid proteolytic degradation of newly synthesized ND1 (30, 31). To evaluate the possibility that FOXRED1 also plays a role as an early complex I assembly factor, we performed a mitochondrial-translation experiment. This showed that the rate of synthesis of all mtDNA-encoded polypeptides in FOXRED1 patient myoblasts was slightly reduced compared to the control; however, the translation profile of the rescued patient cell line (Patient+FR1) remained unchanged, demonstrating that this phenotype was unrelated to the mutant FOXRED1 (Fig. 5C).

FOXRED1 coimmunoprecipitates with several complex I structural subunits and the assembly factors ACAD9 and AIFM1. To identify protein partners that might interact with FOXRED1, we performed immunoprecipitation experiments on a myoblast line expressing FOXRED1-Myc. To verify that the Myc-tagged version of FOXRED1 did not affect the mitochondrial localization of FOXRED1, we performed immunofluorescence

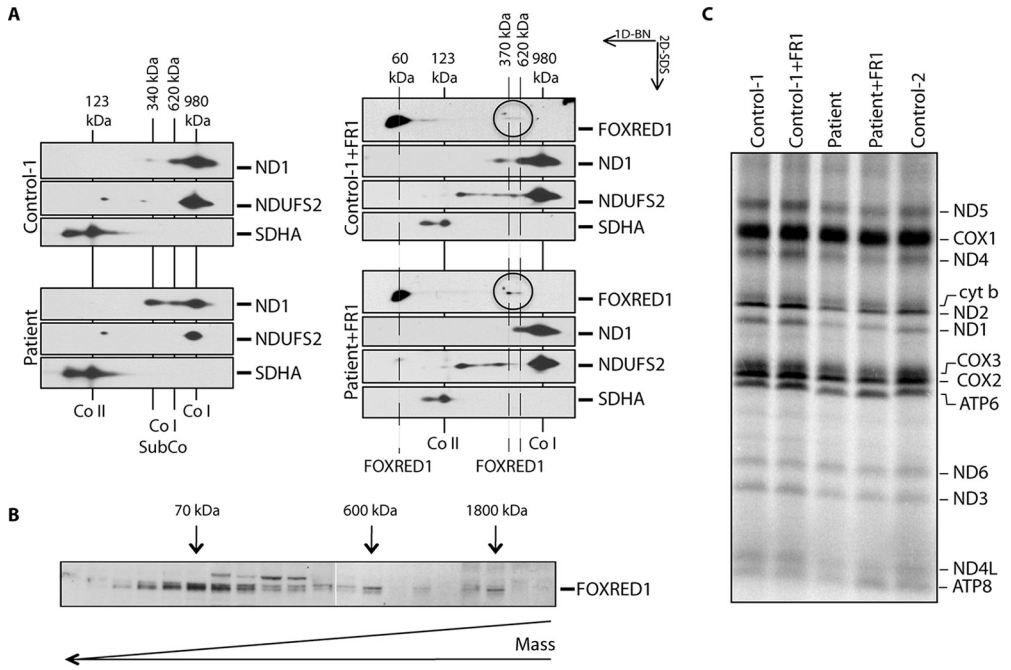

FIG 5 Analysis of FOXRED1 association with complex I intermediates. (A) 2D-SDS-PAGE analysis of a FOXRED1 patient cell line (loaded with twice the amount of total protein), a patient cell line overexpressing wild-type FOXRED1 (Patient+FR1), and controls (Control-1 and Control-1+FR1). The solid lines indicate complexes I and II and complex I subcomplexes. The dashed lines indicate FOXRED1 complexes. OXPHOS complexes were detected with subunit-specific antibodies: Co I, ND1 and NDUFS2; Co II, SDHA. (B) Size exclusion chromatography in control mitochondria from a fibroblast line. The collected fractions were analyzed by SDS-PAGE and immunoblotted with a FOXRED1 antibody. Molecular masses are indicated for fractions in which FOXRED1 was detected. (C) Pulse-labeling of mitochondrially encoded polypeptides with [^{35}S]methionine-cysteine in the FOXRED1 patient myoblast line (Patient), the patient cell line overexpressing wild-type FOXRED1 (Patient+FR1), and three different controls (Control-1, Control-1+FR1, and Control-2). The positions of the ND subunits of complex I, the COX subunits of complex IV, the cytochrome *b* (cyt b) subunit of complex III, and the ATP subunits of complex V are indicated on the right.

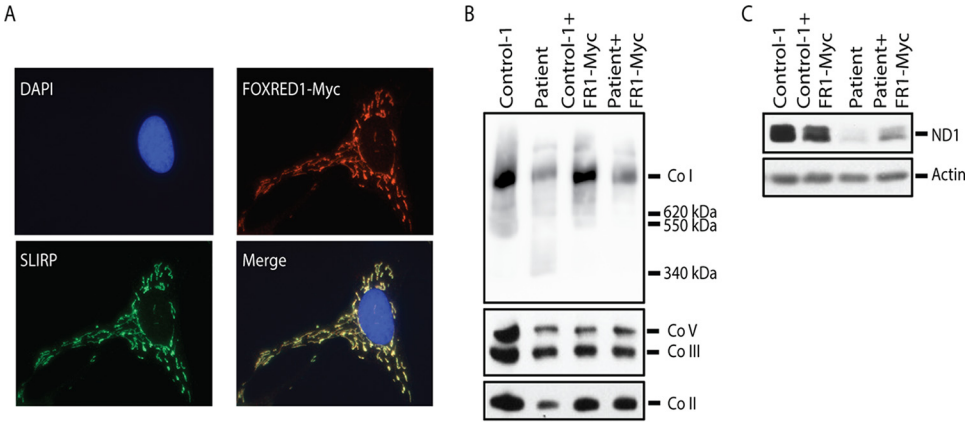

FIG 6 Analysis of the FOXRED1-Myc myoblast line. (A) Immunofluorescence analysis of the FOXRED1-Myc cell line. Antibodies against Myc (red), SLIRP (green), and DAPI (blue) were used for visualization of FOXRED1, mitochondria, and the nucleus, respectively. (B) BN-PAGE analysis of the patient (Patient and Patient+FR1-Myc) and control (Control-1 and Control-1+FR1-Myc) cell lines. OXPHOS complexes were detected with subunit-specific antibodies: Co I, ND1; Co II, SDHA; Co III, UQCRC1; and Co V, ATPase α. (C) SDS-PAGE analysis of the patient (Patient and Patient+FR1-Myc) and control (Control-1 and Control-1+FR1-Myc) cell lines. The immunoblots show the steady-state levels of ND1 and actin (loading control).

experiments to confirm that FOXRED1-Myc was targeted to mitochondria (Fig. 6A). We next tested whether FOXRED1-Myc could rescue the defect observed in the FOXRED1 patient. Immunoblotting showed that the Myc-tagged form of FOXRED1 partially rescued the complex I deficiency in the patient myoblast line and fully rescued the defect in complex II (Fig. 6B). To further evaluate the phenotype observed in the Patient+FOXRED1-Myc cell line, we performed an immunoblot experiment, which confirmed that expression of FOXRED1-Myc in the patient partially rescued the defect observed in ND1 steady-state levels (Fig. 6C).

Mass spectrometry analysis of the elution fraction allowed us to identify a number of proteins that coimmunoprecipitated with FOXRED1, including several nucleus-encoded structural subunits of complex I (NDUFA9, NDUFV1, NDUFB10, NDUFS6, NDUFA11, and NDUFA13) and two complex I assembly factors, AIFM1 and ACAD9. We did not identify any structural components of complex II, but we did find one of the subunits of complex III (UQCRC1) and one subunit of the electron transfer flavoprotein complex (ETFB). We also identified several proteins involved in lipid metabolism: ACSL3, AGPS, HSD17B12, ECI2, ACAD10, AGK, and components of the mitochondrial import machinery and mitochondrial proteases (LONP1, SAMM50, PMCPB, CLPX, TIMM17B, and AFG3L2) (see Table S1 in the supplemental material).

To investigate a putative link between the electron transfer flavoprotein complex (ETF) and the phenotype observed in the FOXRED1 patient cell line, we performed immunoblot analysis of the ETFB protein. SDS-PAGE analysis showed no difference between the steady-state levels of ETFB in the patient cell line and those in controls (Fig. 7A). BN-PAGE analysis detected the ETFB subunit at 70 kDa and 140 kDa, presumably the heterodimer with the ETFA subunit and the dimer plus ETF dehydrogenase (ETFDH), respectively. The steady-state levels of both complexes remained unaffected in FOXRED1-depleted cell lines compared to controls (Fig. 7B).

DISCUSSION

In this study, we identified a homozygous missense mutation in FOXRED1 in a myoblast line from a patient with severe encephalopathy. The two previously reported FOXRED1 patients pre-

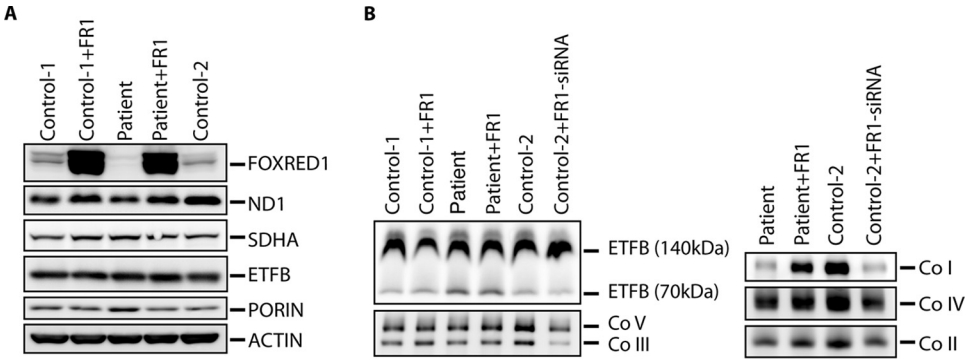

FIG 7 Analysis of ETFB in FOXRED1-depleted cell lines. (A) SDS-PAGE analysis of the patient (Patient and Patient+FR1) and control (Control-1, Control-1+FR1, and Control-2) cell lines. The immunoblots show the steady-state levels of FOXRED1, complex I (ND1), and complex II (SDHA) structural subunits; an ETF subunit (ETFB); and loading controls (porin and actin). (B) BN-PAGE analysis of the FOXRED1 patient cell lines (Patient and Patient+FR1), controls (Control-1, Control-1+FR1, and Control-2), and knockdown of FOXRED1 in Control-2 (Control-2+FR1-siRNA). OXPHOS complexes were detected with subunit-specific antibodies: Co I, ND1; Co II, SDHA; Co III, UQCRC1; Co IV, COX4; and Co V, ATPase α.

sented with infantile-onset encephalomyopathy (19) and Leigh syndrome (13), both associated with a marked, isolated complex I deficiency. Biochemical characterization of our patient myoblast line and a control myoblast line in which FOXRED1 was depleted with siRNA revealed deficient assembly of both complexes I and II, suggesting that the accessory function of FOXRED1 in the assembly of the OXPHOS complexes is both broader than previously appreciated and tissue specific.

The most pronounced defect observed due to loss of FOXRED1 function, however, was a reduction in the amount of fully assembled complex I. The assembly pathway of complex I initiates with the formation of two independent subcomplexes, one membrane module containing the mitochondrially encoded subunit ND1 and the assembly factor NDUFAF5 (7, 9, 30, 32) and another containing the soluble proteins NDUFS2 and NDUFS3 and assembly factors NUBPL, NDUFAF3, NDUFAF4, NDUFAF6, and NDUFAF7 (7, 30, 31, 33). Next, subunits NDUFS7 and NDUFS8, and probably NDUFA9, join the soluble module, forming a 200-kDa subcomplex. This step is followed by the addition of NDUFA3, NDUFA5, NDUFA8, NDUFA12, and NDUFA13 and the assembly factor C3orf1 (17). The combination of these two subassemblies generates a membrane-anchored subcomplex of about 315 kDa. Next, a 370-kDa membrane subcomplex that includes ND2, ND3, ND4L, ND6, NDUFB6, and NDUFB8 structural subunits assembles separately, and at this point, NDUFAF1, ECSIT, ACAD9, and TMEM126B join the assembly pathway (34). The 370- and 315-kDa subcomplexes then assemble to form a 550-kDa subcomplex. This step is followed by the addition of the most distal components of the membrane arm, the mitochondrially encoded subunits ND4, ND5, and NDUFC2, forming the 815-kDa subassembly. The final step requires the presence of the late assembly factor NDUFAF2 and involves the addition of the distal region of the peripheral arm containing the subunits NDUFS1, NDUFS4, NDUFS6, NDUFV1, NDUFV2, and NDUFV3, with the simultaneous addition of subunits NDUFS5, NDUFA1, NDUFA2, NDUFA6, and NDUFA10 (reviewed in references 17, 35, and 36). Our data suggest that FOXRED1 is necessary for promoting the assembly of the 550-kDa subcomplex from the 370-kDa and 315- kDa subcomplexes, as the mutation in, or depletion of, FOXRED1 results in the accumulation of a subassembly that appears as a smear around 340 kDa, which we interpret as an accumulation of the 315- and 370-kDa complexes. We cannot unequivocally determine if the subassembly centered at 340 kDa represents an intermediate on the assembly pathway or a breakdown product that results from a failure to assemble the holoenzyme complex. Our results contrast with those of a recent analysis of FOXRED1 in which an ~475-kDa subcomplex was shown to accumulate in patient fibroblasts, thought to be a result of the breakdown of the late-stage 815-kDa intermediate (20). The reasons for this difference are not immediately clear; however, it is possible that it reflects the difficulty in assigning accurate molecular masses to subassemblies on BN-PAGE gels. A recent careful analysis of complex I subassemblies reassigned the molecular masses of previously reported subcomplexes of 400, 460, 650, and 830 kDa to 315, 370, 550, and 815 kDa, respectively (17). Thus, it is possible that the subassembly we report here is the same as one reported previously (20).

FOXRED1 coimmunoprecipitated with acyl coenzyme A (acyl-CoA) dehydrogenase 9 (ACAD9), a complex I assembly factor that associates with the 370-, 550-, and 815-kDa complex I intermediates (15, 17). Stable isotope labeling using amino acids in cell culture (SILAC) analysis of an NDUFA11-depleted cell line that accumulates the 550- and 815-kDa subcomplexes also showed that the assembly factors ACAD9 and FOXRED1 are involved in the assembly of common intermediates (17). AIFM1, another putative complex I assembly factor, was also identified in the FOXRED1 immunoprecipitation experiment. AIFM1-deficient mouse cells and siRNA-treated HeLa cells showed deficiencies in complex I activity and decreases in the steady-state levels of several complex I structural subunits, *viz.*, NDUFA9, NDUFB6, and NDUFS7 (18, 37).

The size exclusion experiment showed that FOXRED1 appears in higher-molecular-mass complexes, including two peaks corresponding to ~600 kDa and ~1.8 MDa. FOXRED1 coimmunoprecipitates with several proteins involved in complex I biogenesis and with the structural subunit of complex III, UQCRC1. Together, these results raise the possibility that FOXRED1 is also associated with, or involved in the formation of, supercomplexes containing complexes I and III. The presence of FOXRED1 in an ~600-kDa subcomplex (Fig. 5A and B) and the defect in the ND1-containing subcomplex of 620 kDa observed in the FOXRED1 siRNA cell line (Fig. 4A) indicate that FOXRED1 might also play a role in the formation/stability of this subcomplex.

In addition to the complex I deficiency, we also detected a decrease in the steady-state levels of complex II in patient myoblasts, a phenotype not observed in previously described FOXRED1 mutant fibroblast lines (13, 19). Patients with mutations in the complex II structural subunit SDHD also showed a milder defect in complex II in fibroblasts than in myoblasts (38). Four assembly factors of complex II that are conserved in yeast and mammals have been identified. Two of them, SDHAF2 and SDHAF4, are involved in the flavination of SDHA. SDH5 is the yeast homolog of SDHAF2, and an *sdh5*Δ deletion strain showed complete loss of FAD cofactor attachment of SDH1 (the *Saccharomyces cerevisiae* homolog of SDHA). Interestingly, the steady-state levels of nonflavinated SDH1 remained unaffected compared to the control (27). We found no evidence for an alteration in flavinated SDHA in the FOXRED1 patient myoblasts, so the molecular basis for the complex II assembly defect remains unknown.

What could be the connection between the complex I and II assembly defects associated with loss of FOXRED1 function? FOXRED1 contains a domain (pfam01266:DAO) involved in the oxidation/reduction of FAD (39, 40). A phylogenetic analysis of FOXRED1 showed that while all metazoans harboring complex I also have FOXRED1, it is absent in aerobic fungi with a complex I (39). Furthermore, some organisms lacking complex I have FOXRED1. These results suggest that FOXRED1 has a metabolic function that is not always coupled with complex I biogenesis. Complexes I and II are the only OXPHOS complexes that are functionally dependent on FAD. Two electrons generated by the oxidation of NADH in complex I are transferred, one by one, via the FMN, which is noncovalently bound to NDUFV1, and the seven iron sulfur clusters bound to ubiquinone (41). Although FOXRED1 coimmunoprecipitates with the flavinated subunit of complex I, NDUFV1, neither the size exclusion nor the 2D-SDS-PAGE experiments detect FOXRED1 associated with the 815-kDa subcomplex, the step at which the NDUFV1 subunit joins the assembly pathway. Similarly, the immunoprecipitation experi-

ment with FOXRED1 failed to identify any structural subunit or known assembly factor of complex II.

The two assembly factors of complex I that coimmunoprecipitated with FOXRED1 are also FAD dependent. AIFM1 is a flavoprotein with NADH oxidase activity (42), and ACAD9 uses riboflavin, the vitamin precursor of FAD, as a catalytic cofactor. The FOXRED1 immunoprecipitation experiment identified several enzymes involved in lipid metabolism, including the electron transfer flavoprotein beta polypeptide, ETFB; however, we did not observe any alterations in the level of this protein in patient myoblasts. The beta-oxidation of lipids has as it central reaction acyl-CoA dehydrogenation, which generates acetyl-CoA, $FADH_2$, and NADH. The supply of some of these reducing equivalents to the respiratory chain is performed by ETF and ETFDH (43). These observations illustrate a potential, but still speculative, link between FOXRED1 and flavin metabolism.

Together, our results suggest that FOXRED1 plays a role in the assembly of complex I by associating with the ~370-kDa subcomplex and the FAD-dependent assembly factor ACAD9, and probably AIFM1. Depletion of FOXRED1 expression results in a severe defect in the formation of the 550-kDa subcomplex. Additional work will be required to determine the precise roles of FOXRED1 in the assembly pathways of both complexes I and II.

ACKNOWLEDGMENT

We declare no conflict of interest.

FUNDING INFORMATION

This work, including the efforts of Olga Zurita Rendón, was funded by Consejo Nacional de Ciencia y Tecnología (CONACYT) (209378). This work, including the efforts of Eric Alan Shoubridge, was funded by Gouvernement du Canada | Canadian Institutes of Health Research (CIHR). This work, including the efforts of Olga Zurita Rendón, was funded by Fonds de Recherche du Québec—Nature et Technologies (FRQNT) (140802).

REFERENCES

1. **Lazarou M, Thorburn DR, Ryan MT, McKenzie M.** 2009. Assembly of mitochondrial complex I and defects in disease. Biochim Biophys Acta **1793:**78–88. http://dx.doi.org/10.1016/j.bbamcr.2008.04.015.
2. **Distelmaier F, Koopman WJ, van den Heuvel LP, Rodenburg RJ, Mayatepek E, Willems PH, Smeitink JA.** 2009. Mitochondrial complex I deficiency: from organelle dysfunction to clinical disease. Brain **132:**833–842. http://dx.doi.org/10.1093/brain/awp058.
3. **Thorburn DR.** 2004. Mitochondrial disorders: prevalence, myths and advances. J Inherit Metab Dis **27:**349–362. http://dx.doi.org/10.1023/B:BOLI.0000031098.41409.55.
4. **Janssen RJ, Nijtmans LG, van den Heuvel LP, Smeitink JA.** 2006. Mitochondrial complex I: structure, function and pathology. J Inherit Metab Dis **29:**499–515. http://dx.doi.org/10.1007/s10545-006-0362-4.
5. **Vogel RO, Janssen RJ, Ugalde C, Grovenstein M, Huijbens RJ, Visch HJ, van den Heuvel LP, Willems PH, Zeviani M, Smeitink JA, Nijtmans LG.** 2005. Human mitochondrial complex I assembly is mediated by NDUFAF1. FEBS J **272:**5317–5326. http://dx.doi.org/10.1111/j.1742-4658.2005.04928.x.
6. **Ogilvie I, Kennaway NG, Shoubridge EA.** 2005. A molecular chaperone for mitochondrial complex I assembly is mutated in a progressive encephalopathy. J Clin Invest **115:**2784–2792. http://dx.doi.org/10.1172/JCI26020.
7. **Saada A, Vogel RO, Hoefs SJ, van den Brand MA, Wessels HJ, Willems PH, Venselaar H, Shaag A, Barghuti F, Reish O, Shohat M, Huynen MA, Smeitink JA, van den Heuvel LP, Nijtmans LG.** 2009. Mutations in NDUFAF3 (C3ORF60), encoding an NDUFAF4 (C6ORF66)-interacting complex I assembly protein, cause fatal neonatal mitochondrial disease. Am J Hum Genet **84:**718–727. http://dx.doi.org/10.1016/j.ajhg.2009.04.020.
8. **Saada A, Edvardson S, Rapoport M, Shaag A, Amry K, Miller C, Lorberboum-Galski H, Elpeleg O.** 2008. C6ORF66 is an assembly factor of mitochondrial complex I. Am J Hum Genet **82:**32–38. http://dx.doi.org/10.1016/j.ajhg.2007.08.003.
9. **Sugiana C, Pagliarini DJ, McKenzie M, Kirby DM, Salemi R, Abu-Amero KK, Dahl HH, Hutchison WM, Vascotto KA, Smith SM, Newbold RF, Christodoulou J, Calvo S, Mootha VK, Ryan MT, Thorburn DR.** 2008. Mutation of C20orf7 disrupts complex I assembly and causes lethal neonatal mitochondrial disease. Am J Hum Genet **83:**468–478. http://dx.doi.org/10.1016/j.ajhg.2008.09.009.
10. **Pagliarini DJ, Calvo SE, Chang B, Sheth SA, Vafai SB, Ong SE, Walford GA, Sugiana C, Boneh A, Chen WK, Hill DE, Vidal M, Evans JG, Thorburn DR, Carr SA, Mootha VK.** 2008. A mitochondrial protein compendium elucidates complex I disease biology. Cell **134:**112–123. http://dx.doi.org/10.1016/j.cell.2008.06.016.
11. **Vogel RO, Janssen RJ, van den Brand MA, Dieteren CE, Verkaart S, Koopman WJ, Willems PH, Pluk W, van den Heuvel LP, Smeitink JA, Nijtmans LG.** 2007. Cytosolic signaling protein Ecsit also localizes to mitochondria where it interacts with chaperone NDUFAF1 and functions in complex I assembly. Genes Dev **21:**615–624. http://dx.doi.org/10.1101/gad.408407.
12. **Rhein VF, Carroll J, Ding S, Fearnley IM, Walker JE.** 2013. NDUFAF7 methylates arginine 85 in the NDUFS2 subunit of human complex I. J Biol Chem **288:**33016–33026. http://dx.doi.org/10.1074/jbc.M113.518803.
13. **Calvo SE, Tucker EJ, Compton AG, Kirby DM, Crawford G, Burtt NP, Rivas M, Guiducci C, Bruno DL, Goldberger OA, Redman MC, Wiltshire E, Wilson CJ, Altshuler D, Gabriel SB, Daly MJ, Thorburn DR, Mootha VK.** 2010. High-throughput, pooled sequencing identifies mutations in NUBPL and FOXRED1 in human complex I deficiency. Nat Genet **42:**851–858. http://dx.doi.org/10.1038/ng.659.
14. **Bych K, Kerscher S, Netz DJ, Pierik AJ, Zwicker K, Huynen MA, Lill R, Brandt U, Balk J.** 2008. The iron-sulphur protein Ind1 is required for effective complex I assembly. EMBO J **27:**1736–1746. http://dx.doi.org/10.1038/emboj.2008.98.
15. **Nouws J, Nijtmans L, Houten SM, van den Brand M, Huynen M, Venselaar H, Hoefs S, Gloerich J, Kronick J, Hutchin T, Willems P, Rodenburg R, Wanders R, van den Heuvel L, Smeitink J, Vogel RO.** 2010. Acyl-CoA dehydrogenase 9 is required for the biogenesis of oxidative phosphorylation complex I. Cell Metab **12:**283–294. http://dx.doi.org/10.1016/j.cmet.2010.08.002.
16. **Heide H, Bleier L, Steger M, Ackermann J, Drose S, Schwamb B, Zornig M, Reichert AS, Koch I, Wittig I, Brandt U.** 2012. Complexome profiling identifies TMEM126B as a component of the mitochondrial complex I assembly complex. Cell Metab **16:**538–549. http://dx.doi.org/10.1016/j.cmet.2012.08.009.
17. **Andrews B, Carroll J, Ding S, Fearnley IM, Walker JE.** 2013. Assembly factors for the membrane arm of human complex I. Proc Natl Acad Sci U S A **110:**18934–18939. http://dx.doi.org/10.1073/pnas.1319247110.
18. **Vahsen N, Cande C, Briere JJ, Benit P, Joza N, Larochette N, Mastroberardino PG, Pequignot MO, Casares N, Lazar V, Feraud O, Debili N, Wissing S, Engelhardt S, Madeo F, Piacentini M, Penninger JM, Schagger H, Rustin P, Kroemer G.** 2004. AIF deficiency compromises oxidative phosphorylation. EMBO J **23:**4679–4689. http://dx.doi.org/10.1038/sj.emboj.7600461.
19. **Fassone E, Duncan AJ, Taanman JW, Pagnamenta AT, Sadowski MI, Holand T, Qasim W, Rutland P, Calvo SE, Mootha VK, Bitner-Glindzicz M, Rahman S.** 2010. FOXRED1, encoding an FAD-dependent oxidoreductase complex-I-specific molecular chaperone, is mutated in infantile-onset mitochondrial encephalopathy. Hum Mol Genet **19:**4837–4847. http://dx.doi.org/10.1093/hmg/ddq414.
20. **Formosa LE, Mimaki M, Frazier AE, McKenzie M, Stait TL, Thorburn DR, Stroud DA, Ryan MT.** 2015. Characterization of mitochondrial FOXRED1 in the assembly of respiratory chain complex I. Hum Mol Genet **24:**2952–2965. http://dx.doi.org/10.1093/hmg/ddv058.
21. **Lochmuller H, Johns T, Shoubridge EA.** 1999. Expression of the E6 and E7 genes of human papillomavirus (HPV16) extends the life span of human myoblasts. Exp Cell Res **248:**186–193. http://dx.doi.org/10.1006/excr.1999.4407.
22. **Klement P, Nijtmans LG, Van den Bogert C, Houstek J.** 1995. Analysis of oxidative phosphorylation complexes in cultured human fibroblasts and amniocytes by blue-native-electrophoresis using mitoplasts isolated

with the help of digitonin. Anal Biochem **231:**218–224. http://dx.doi.org/10.1006/abio.1995.1523.
23. **Schagger H, von Jagow G.** 1991. Blue native electrophoresis for isolation of membrane protein complexes in enzymatically active form. Anal Biochem **199:**223–231. http://dx.doi.org/10.1016/0003-2697(91)90094-A.
24. **Wittig I, Beckhaus T, Wumaier Z, Karas M, Schagger H.** 2010. Mass estimation of native proteins by blue native electrophoresis: principles and practical hints. Mol Cell Proteomics **9:**2149–2161. http://dx.doi.org/10.1074/mcp.M900526-MCP200.
25. **Kaufman BA, Durisic N, Mativetsky JM, Costantino S, Hancock MA, Grutter P, Shoubridge EA.** 2007. The mitochondrial transcription factor TFAM coordinates the assembly of multiple DNA molecules into nucleoid-like structures. Mol Biol Cell **18:**3225–3236. http://dx.doi.org/10.1091/mbc.E07-05-0404.
26. **Sasarman F, Shoubridge EA.** 2012. Radioactive labeling of mitochondrial translation products in cultured cells. Methods Mol Biol **837:**207–217. http://dx.doi.org/10.1007/978-1-61779-504-6_14.
27. **Hao HX, Khalimonchuk O, Schraders M, Dephoure N, Bayley JP, Kunst H, Devilee P, Cremers CW, Schiffman JD, Bentz BG, Gygi SP, Winge DR, Kremer H, Rutter J.** 2009. SDH5, a gene required for flavination of succinate dehydrogenase, is mutated in paraganglioma. Science **325:**1139–1142. http://dx.doi.org/10.1126/science.1175689.
28. **Bafunno V, Giancaspero TA, Brizio C, Bufano D, Passarella S, Boles E, Barile M.** 2004. Riboflavin uptake and FAD synthesis in Saccharomyces cerevisiae mitochondria: involvement of the Flx1p carrier in FAD export. J Biol Chem **279:**95–102. http://dx.doi.org/10.1074/jbc.M308230200.
29. **Antonicka H, Mattman A, Carlson CG, Glerum DM, Hoffbuhr KC, Leary SC, Kennaway NG, Shoubridge EA.** 2003. Mutations in COX15 produce a defect in the mitochondrial heme biosynthetic pathway, causing early-onset fatal hypertrophic cardiomyopathy. Am J Hum Genet **72:**101–114. http://dx.doi.org/10.1086/345489.
30. **Zurita Rendon O, Shoubridge EA.** 2012. Early complex I assembly defects result in rapid turnover of the ND1 subunit. Hum Mol Genet **21:**3815–3824. http://dx.doi.org/10.1093/hmg/dds209.
31. **Zurita Rendon O, Silva Neiva L, Sasarman F, Shoubridge EA.** 2014. The arginine methyltransferase NDUFAF7 is essential for complex I assembly and early vertebrate embryogenesis. Hum Mol Genet **23:**5159–5170. http://dx.doi.org/10.1093/hmg/ddu239.
32. **Gerards M, Sluiter W, van den Bosch BJ, de Wit LE, Calis CM, Frentzen M, Akbari H, Schoonderwoerd K, Scholte HR, Jongbloed RJ, Hendrickx AT, de Coo IF, Smeets HJ.** 2010. Defective complex I assembly due to C20orf7 mutations as a new cause of Leigh syndrome. J Med Genet **47:**507–512. http://dx.doi.org/10.1136/jmg.2009.067553.
33. **Vogel RO, Dieteren CE, van den Heuvel LP, Willems PH, Smeitink JA, Koopman WJ, Nijtmans LG.** 2007. Identification of mitochondrial complex I assembly intermediates by tracing tagged NDUFS3 demonstrates the entry point of mitochondrial subunits. J Biol Chem **282:**7582–7590.
34. **Perales-Clemente E, Fernandez-Vizarra E, Acin-Perez R, Movilla N, Bayona-Bafaluy MP, Moreno-Loshuertos R, Perez-Martos A, Fernandez-Silva P, Enriquez JA.** 2010. Five entry points of the mitochondrially encoded subunits in mammalian complex I assembly. Mol Cell Biol **30:**3038–3047. http://dx.doi.org/10.1128/MCB.00025-10.
35. **Mimaki M, Wang X, McKenzie M, Thorburn DR, Ryan MT.** 2012. Understanding mitochondrial complex I assembly in health and disease. Biochim Biophys Acta **1817:**851–862. http://dx.doi.org/10.1016/j.bbabio.2011.08.010.
36. **McKenzie M, Ryan MT.** 2010. Assembly factors of human mitochondrial complex I and their defects in disease. IUBMB Life **62:**497–502. http://dx.doi.org/10.1002/iub.335.
37. **Cheung EC, Joza N, Steenaart NA, McClellan KA, Neuspiel M, McNamara S, MacLaurin JG, Rippstein P, Park DS, Shore GC, McBride HM, Penninger JM, Slack RS.** 2006. Dissociating the dual roles of apoptosis-inducing factor in maintaining mitochondrial structure and apoptosis. EMBO J **25:**4061–4073. http://dx.doi.org/10.1038/sj.emboj.7601276.
38. **Jackson CB, Nuoffer JM, Hahn D, Prokisch H, Haberberger B, Gautschi M, Haberli A, Gallati S, Schaller A.** 2014. Mutations in SDHD lead to autosomal recessive encephalomyopathy and isolated mitochondrial complex II deficiency. J Med Genet **51:**170–175. http://dx.doi.org/10.1136/jmedgenet-2013-101932.
39. **Lemire BD.** 2015. Evolution of FOXRED1, an FAD-dependent oxidoreductase necessary for NADH:ubiquinone oxidoreductase (complex I) assembly. Biochim Biophys Acta **1847:**451–457. http://dx.doi.org/10.1016/j.bbabio.2015.01.014.
40. **Lemire BD.** 2015. A structural model for FOXRED1, an FAD-dependent oxidoreductase necessary for NADH: ubiquinone oxidoreductase (complex I) assembly. Mitochondrion **22:**9–16. http://dx.doi.org/10.1016/j.mito.2015.02.008.
41. **Baradaran R, Berrisford JM, Minhas GS, Sazanov LA.** 2013. Crystal structure of the entire respiratory complex I. Nature **494:**443–448. http://dx.doi.org/10.1038/nature11871.
42. **Susin SA, Lorenzo HK, Zamzami N, Marzo I, Snow BE, Brothers GM, Mangion J, Jacotot E, Costantini P, Loeffler M, Larochette N, Goodlett DR, Aebersold R, Siderovski DP, Penninger JM, Kroemer G.** 1999. Molecular characterization of mitochondrial apoptosis-inducing factor. Nature **397:**441–446. http://dx.doi.org/10.1038/17135.
43. **Gregersen N.** 1985. Riboflavin-responsive defects of beta-oxidation. J Inherit Metab Dis **8**(Suppl 1):S65–S69.